Lagrangian coherent structures in the ocean favourable for fishing grounds

S.V. Prants, M.V. Budyansky, M.Yu. Uleysky

Laboratory of Nonlinear Dynamical Systems
Pacific Oceanological Institute of the Russian Academy of Sciences, Vladivostok, Russia
URL: dynalab.poi.dvo.ru

PICES 2012 Annual Meeting
Hiroshima, Japan, 12–21 October, 2012

Kuroshio-Oyashio frontal zone

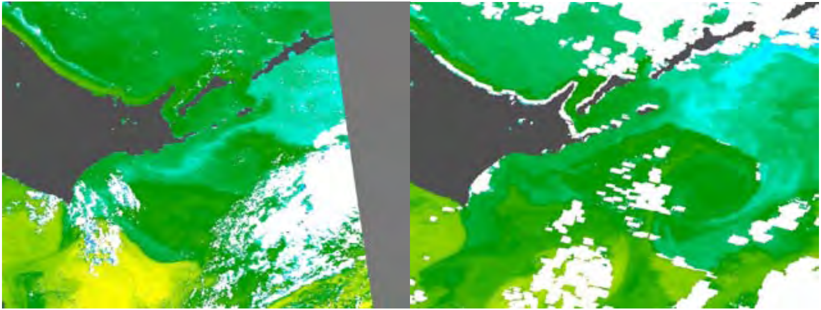

SST images on: (left) 25 September 2002 (the First Oyashio Intrusion) and (right) 12 October 2005 (the Second Oyashio Intrusion).

Pacific saury migration ways

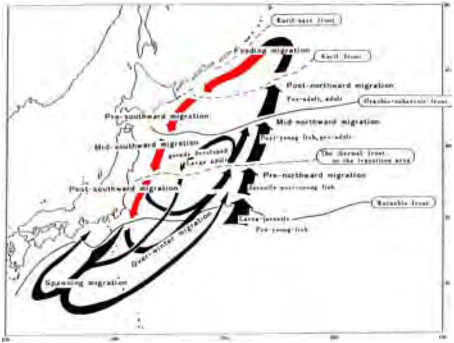

(Kosaka's picture) Saury migrate seasonally from the south to the north. In winter and spring, spawning grounds are off the eastern coast of Honshu (Fukushima, Saitoh, Yasuda et al). In spring and summer, juvenile and young saury migrate northward to the Oyashio area. After feeding, adult saury migrate to the south in the late summer. Commercial fishing: August – December.

What is known

Some species of pelagic fish are known to accumulate for feeding and spawning at oceanic features like fronts, eddies, streamers and upwelling (Uda, Owen, Bakun et al).

In some years saury fishing grounds are formed near Hokkaido shore, while in other years they are located far offshore (Uda, Fukushima, Yasuda, Saitoh, Filatov, Samko, Bulatov et al). Locations of the fishing grounds depend not only on local oceanographic environments around the fishing grounds, but also on oceanographic conditions over an extensive range of the Oyashio area.

The aim

Searching for a connection between **Lagrangian fronts, delineating boundaries between surface waters with different Lagrangian properties**, and fishing grounds with maximal catches of Pacific saury (**Cololabis saira**), one of the most commercial pelagic fishes in the region.

Based on the AVISO altimetric velocity fields, we compute synoptic maps of zonal, meridional and absolute drift of synthetic tracers, their Lyapunov exponents and zonal and meridional entrance maps. Those maps with positions of maximal saury catch overlaid allow to identify the Lagrangian fronts in the region with favourable fishing conditions in the years both with the First and Second Oyashio Intrusions. The Lagrangian fronts may serve a new indicator for potential fishing grounds.

What we solve

Advection equations for millions of tracers in a geostrophic velocity field are integrated forward and backward in time. Integrating (1) forward in time, we know the fate of water masses and backward in time we know their origin and history.

$$\frac{dx}{dt} = u_g(x, y, t), \quad \frac{dy}{dt} = v_g(x, y, t), \tag{1}$$

(x, y) tracer's location, u_g and v_g zonal and meridional components of its velocity. Even if the Eulerian velocity field is fully deterministic, the tracer's trajectories may be very complicated and practically unpredictable. It means that a distance between two initially close tracers grows exponentially in time $\|\delta\mathbf{r}(t)\| = \|\delta\mathbf{r}(0)\| \exp(\lambda t)$, λ is a maximal Lyapunov exponent. The phenomenon known as chaotic advection (Aref). See a review paper "Chaotic advection in the ocean" by Koshel and Prants, Physics – Uspekhi. V.49 N11. (2006) P.1151.

Lagrangian coherent structures in the ocean

Lagrangian coherent structures in a flow are material surfaces dividing a flow in dynamically different regions (Haller). They are material lines in 2D flows. The most important of them are stable and unstable invariant manifolds of hyperbolic (unstable) trajectories.

Streamlines for a steady flow is an example of the invariant manifold. Unsteady chaotic flow possesses an infinite number of hyperbolic trajectories $\gamma_i(t)$. Some of them are the most influential ones.

Stable (W_s) and unstable (W_u) manifolds of a hyperbolic trajectory $\gamma(t)$ are material lines consisting of a set of points through which at time moment t pass trajectories asymptotical to $\gamma(t)$ at $t \to \infty$ (W_s) and $t \to -\infty$ (W_u) (Prants, Wiggins et al).

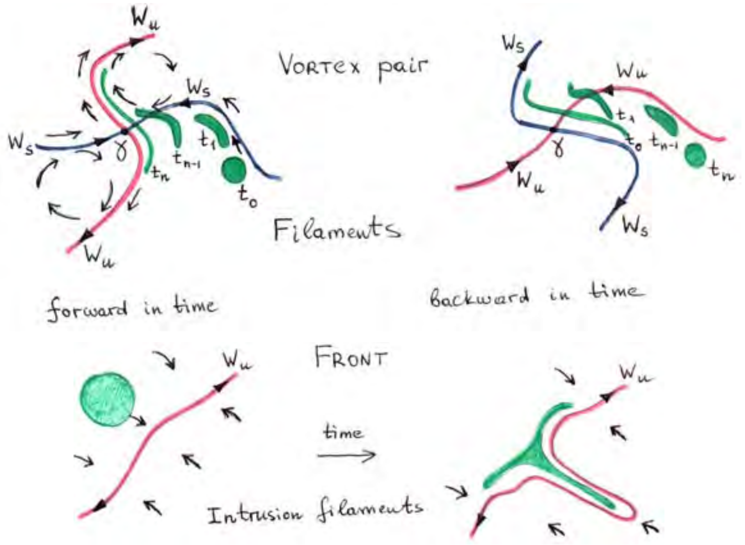
Vortex pair
Filaments
forward in time
backward in time
W_u
W_s
γ
t_0
t_1
t_{n-1}
t_n
Front
time
Intrusion filaments

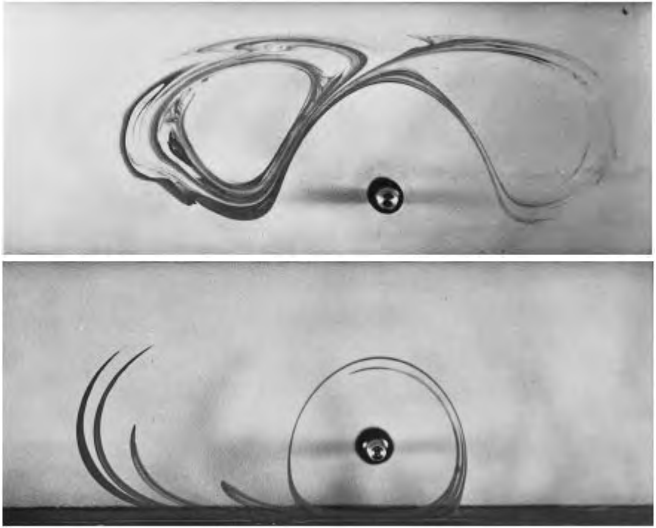

Visualization of the unstable manifolds with a dye in a laboratory flow (Hackborn, 1997).

Stable and unstable manifolds are hidden in a flow, but they are important

1. They form a sceleton in complicated ocean flows and divide them in dynamically different regions.
2. They are in charge of forming an inhomogeneous mixing.
3. They are transport barriers separating water masses with different characteristics.
4. Stable manifolds are repellers and unstable ones are attractors. That is why unstable manifolds may be rich in nutrients being oceanic “dining rooms”.
5. They are Lagrangian fronts.

How to compute and visualize stable and unstable manifolds in oceanic flows?

Finite-time Lyapunov exponents (FTLE)

FTLE is the finite-time average of the maximal separation rate for a pair of neighbouring advected particles.

The FTLE at position $\mathbf{r}$ at time τ is given by (SP et al, Ocean Modelling 2011)

$$\lambda(\mathbf{r}(t)) \equiv \frac{1}{\tau} \ln \sigma(G(t)), \tag{2}$$

τ integration time, $\sigma(G(t))$ the largest singular value of the evolution matrix for linearized advection equations. Scalar field of the FTLE is Eulerian but the very quantity is a Lagrangian one.

Ridges (curves of local maximum) of the FTLE field visualize stable manifolds when integrating advection equations forward in time and unstable ones when integrating them backward in time.

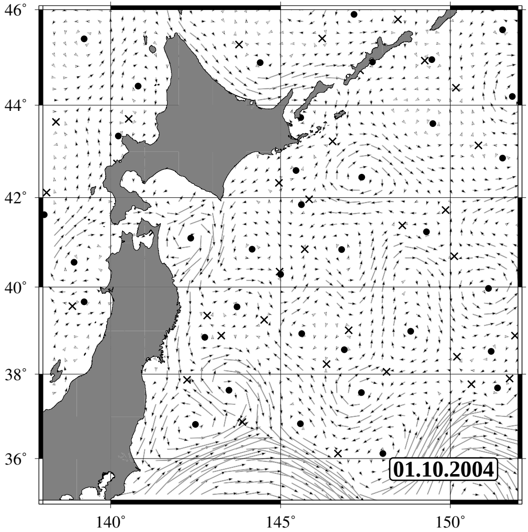

Instantaneous altimetric velocity field in the region with elliptic (circles) and hyperbolic (crosses) points.

Lagrangian fronts

Surface Lagrangian front is a boundary between surface waters with different Lagrangian properties.

1. Any ridge on a Lyapunov map is a Lagrangian front because it separates waters with different mixing properties.
2. The other Lagrangian quantities:
3. Zonal D_x, meridional D_y, and absolute, $D = \sqrt{(x_f - x_0)^2 + (y_f - y_0)^2} \equiv \sqrt{D_x^2 + D_y^2}$, drift of synthetic tracers.
4. Times of entrance, residence and exit of tracers from a given region.
5. Ridges on the corresponding synoptic maps deliniate Lagrangian fronts.

The manifolds at work delineating Lagrangian fronts

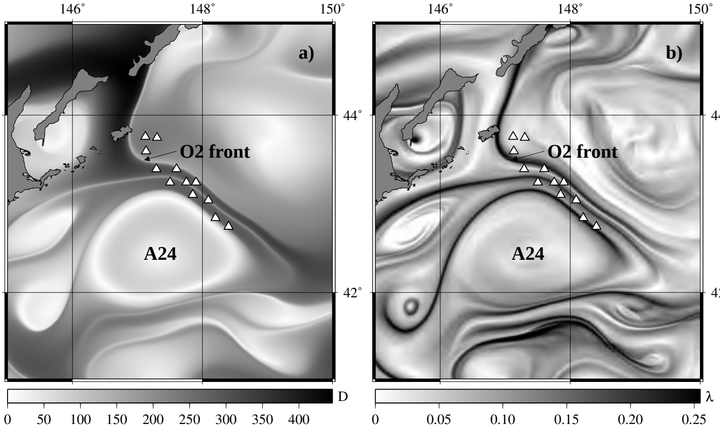

(left) Drift map, $D = \sqrt{(x_f - x_0)^2 + (y_f - y_0)^2}$, and (right) Lyapunov map with saury catch locations on October 1, 2004. Backward-in-time integration for two weeks.

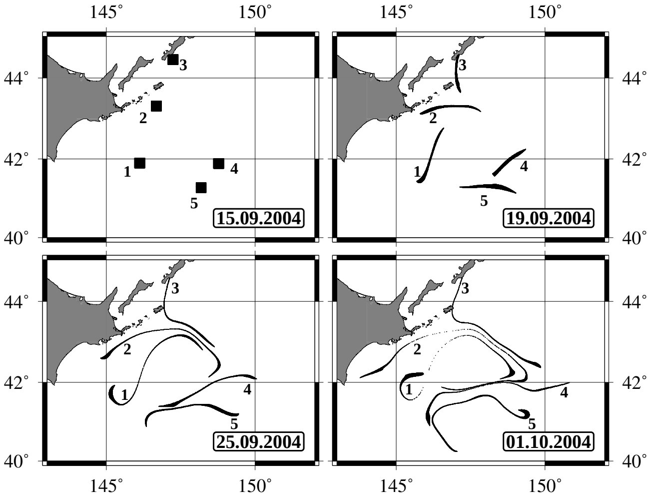

Evolution of the synthetic patches chosen nearby the hyperbolic points in the region. Forward-in-time integration for two weeks. In course of time the patches track the corresponding unstable manifolds.

Lagrangian fronts and three days saury catch locations in the season with the First Oyashio Intrusion

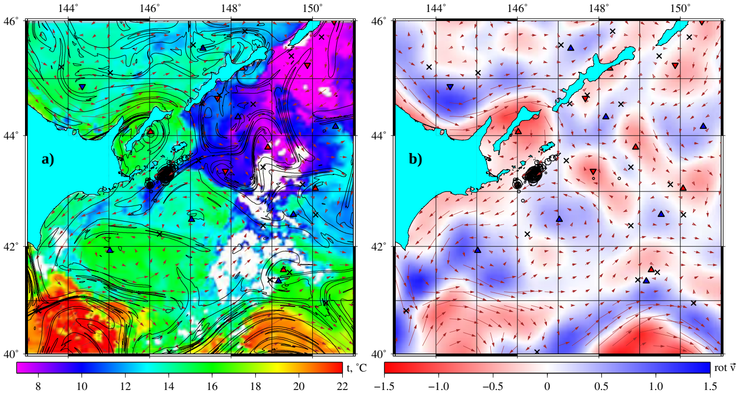

24 September 2002: (a) SST image and (b) vorticity map with locations of saury catches for three days imposed. Circle's radius is proportional to the catch mass per a given ship.

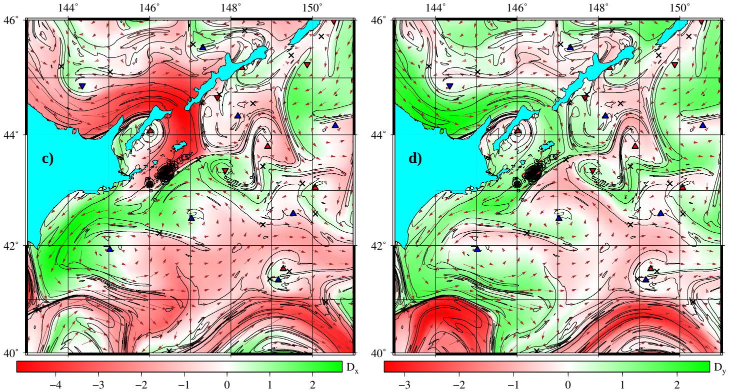

(c) Zonal and (d) meridional drift maps on 24 September 2002. $D_{x,y}$ are in degrees. Backward-in-time integration for two weeks. The Lagrangian front between Soya and Oyashio waters.

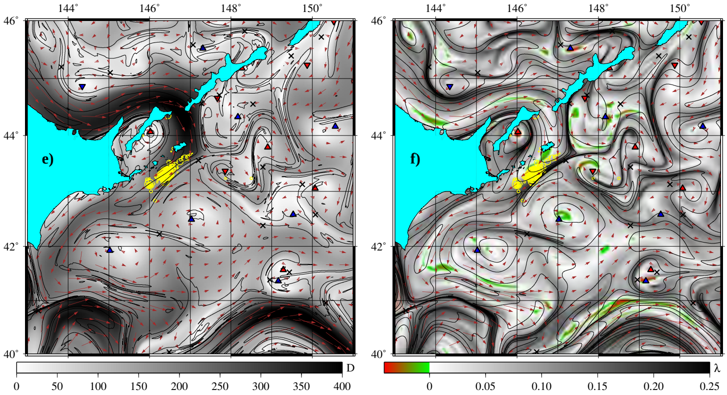

(e) Absolute drift map and (f) FTLE map on 24 September 2002 with locations of saury catches imposed. FTLE is in units of $[\text{days}]^{-1}$ and the absolute drift, D, is in km. Backward-in-time integration for two weeks.

Lagrangian fronts and three days saury catch locations in the season with the Second Oyashio Intrusion

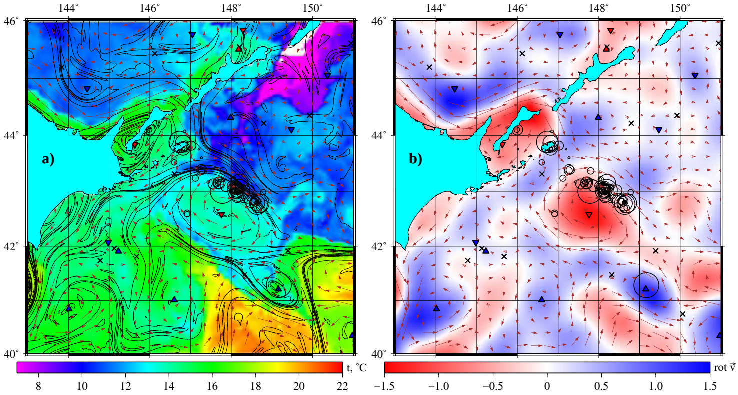

17 October 2004: (a) SST image and (b) vorticity map with locations of saury catches for three days imposed. Circle's radius is proportional to the catch mass per a given ship.

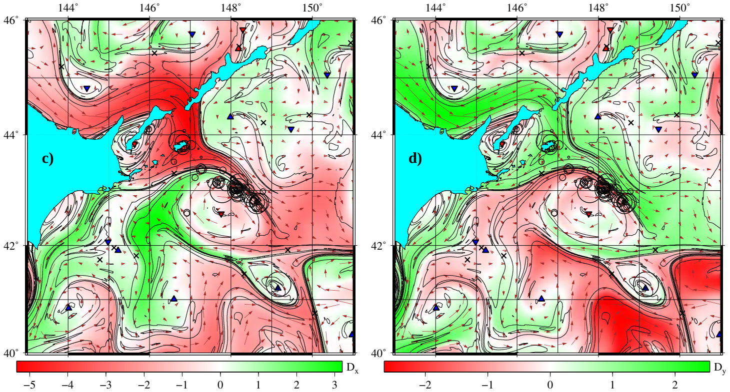

17 October 2004: (c) zonal and (d) meridional drift maps. $D_{x,y}$ are in degrees. Backward-in-time integration for two weeks. The Lagrangian fronts between Soya, Oyashio and Kuroshio waters.

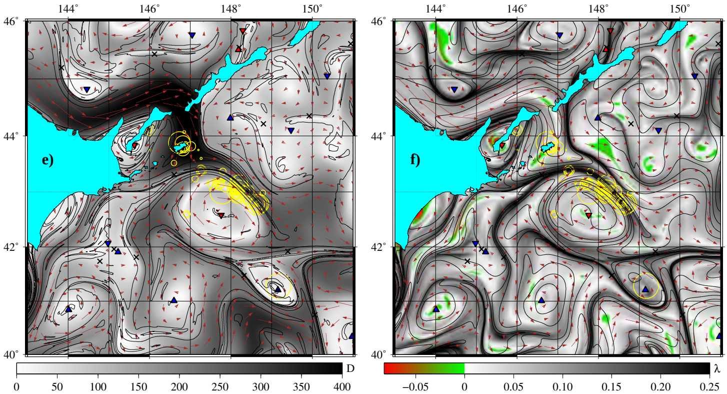

17 October 2004: (e) absolute drift map and (f) FTLE map with locations of saury catches imposed. FTLE is in units of $[\mathrm{days}]^{-1}$ and the absolute drift, D, is in km.

Lagrangian fronts and two weeks saury catch locations in the season with the First Oyashio Intrusion

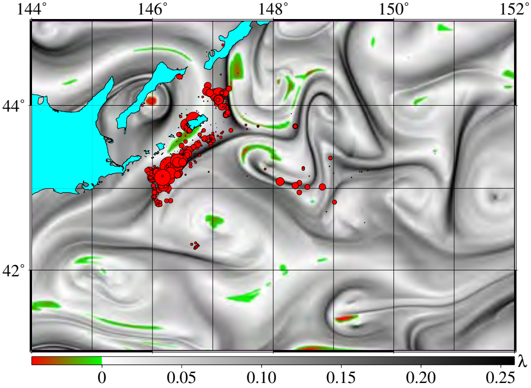

Lyapunov map on September 26, 2002 with cumulative saury catch locations for the period from September, 19 to October, 2. Circle's radius is proportional to the catch mass per a given ship.

Lagrangian fronts and two weeks saury catch locations in the season with the Second Oyashio Intrusion

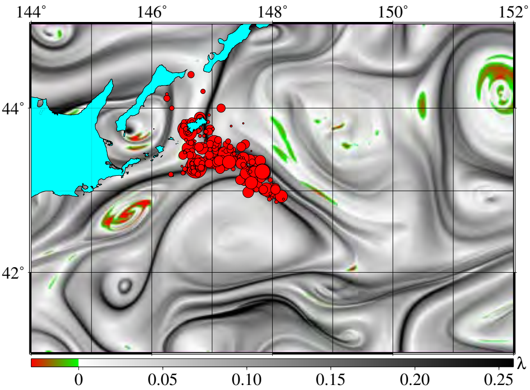

Lyapunov map on October 1, 2004 with cumulative saury catch locations for the period from September, 24 to October, 8. Circle's radius is proportional to the catch mass per a given ship.

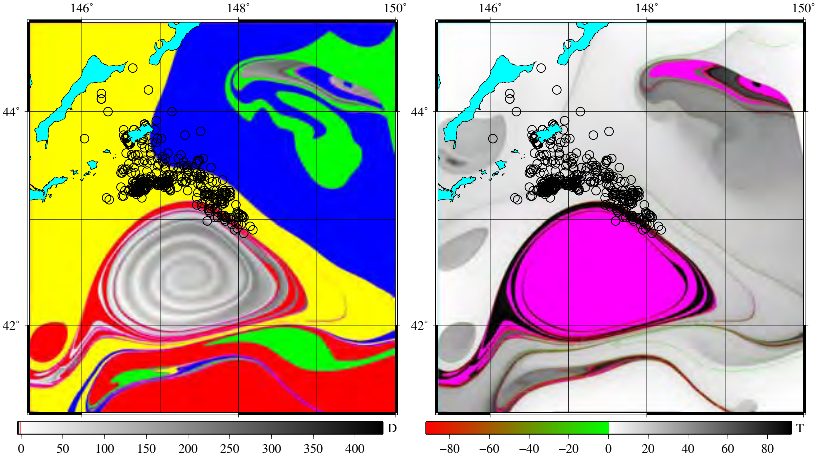

Accurate locations of Lagrangian fronts between Soya, Oyashio and Kuroshio waters. (left) Were the waters came from: yellow – from the west, green – the east, blue – the north, red – the south, grey – the resident waters. (right) Entrance time map.

Forecast of potential saury fishing grounds in September of 2012 with a few catch locations

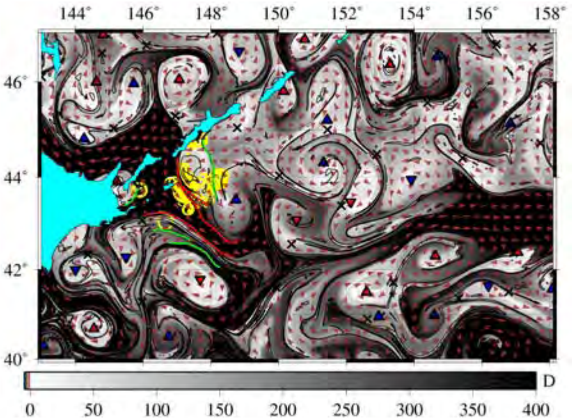

Drift map on September 14, 2012 with locations of saury catches imposed after predicting potential Lagrangian fronts.

What we need to test the method and go ahead

We've used the saury catch data in 2001–2012 provided by the Russian Fishery Agency.

What we need are Japanese data on saury, tuna, squid catch locations and other pelagic fishes.

Largangian fronts are potential fishing grounds: physical reasons

1. The LFs are zones of convergence of waters with different history, origin and properties.
2. They are regions with enhanced physical energy.
3. Downwelling at the LFs favour the accumulation of forage plankton.
4. Upwelling nearby the LFs favour the enhancement of primary production.

Fish cannot "eat" the physical energy, but the enhanced physical energy may create favourable conditions at all trophic levels.

Resume: Lagrangian fronts and potential fishing grounds

1. Based on altimetric velocity fields, we demarcate LFs on computed maps of Lagrangian quantities (Lyapunov exponents, zonal, meridional, absolute drifts, entrance and exit times).
2. Identification of LFs with potential fishing grounds by analyzing oceanic fronts in the region and computed synoptic maps.
3. Correlation between the computed LFs with potential fishing grounds and locations with maximal saury catches.
4. Computed LFs are new indicators for potential fishing grounds.
5. Forecast of potential fishing grounds with the help of computed LFs.
6. The method is quite general and applicable for any region (besides the equatorial one) and different pelagic fishes (tuna, squid, etc.).

Recent publications see at URL: dynalab.poi.dvo.ru

- S.V. Prants, M.Yu. Uleysky, M.V. Budyansky. Lagrangian coherent structures in the ocean with favourable fishery conditions. *Doklady Earth Sciences*. (2012) (in press).
- S.V. Prants, V.I. Ponomarev, M.V. Budyansky, M.Yu. Uleysky, P.A. Fayman. Lagrangian analysis of mixing and transport of water masses in marine bays. *Izvestia Atmos. Oceanic Phys.* (2012) (in press)
- S.V. Prants, M.V. Budyansky, V.I. Ponomarev, M.Yu. Uleysky. Lagrangian study of transport and mixing in a mesoscale eddy street. *Ocean modelling*. V.38, Is.1-2 (2011) 114-125.
- S.V. Prants, M.Yu. Uleysky, M.V. Budyansky. Numerical simulation of propagation of radioactive pollution in the ocean from the Fukushima-Dai-ichi nuclear plant. *Doklady Earth Sciences*. V.439, (2011) 1179-1182.
- M.Yu. Uleysky, M.V. Budyansky, S.V. Prants. Chaotic cross-jet transport in two dimensional flows. *J. Exper. Theor. Phys.* V.111 (2010) 1039-1049.
- M.Yu. Uleysky, M.V. Budyansky, and S.V. Prants. Mechanism of destruction of the transport barriers in geophysical jets with Rossby waves. *Physical Review E*. V.81 (2010) art. no 017202.